Springer

Journal of Mechanical Science and Technology 22 (2008) 2357~2364

Journal of
Mechanical
Science and
Technology

www.springerlink.com/content/1738-494x
DOI: 10.1007/s12206-008-0930-7

Performance limit of a passive vertical isolator using a negative stiffness mechanism †

Hyeong-Joon Ahn*

Department of Mechanical Engineering, Soongsil University, 511 Sangdo-dong, Dongjak-gu, Seoul, Korea, 156-743

(Manuscript Received July 26, 2007; Revised June 24, 2008; Accepted September 26, 2008)

Abstract

A passive vibration isolator using a negative stiffness mechanism (NSM) is being considered for small precision instruments since it does not need any outer power supply and pressurized air, and its fundamental frequency can be lowered down to 0.5 Hz. Although the working principle of the NSM and its patents are well known, neither the isolation performance limit related to the lowest fundamental frequency nor its nonlinear behavior have been studied. This paper discusses the performance limit of the passive vertical isolator using the NSM and presents the design guidelines for the isolator based on that performance limit. First, a nonlinear dynamic model of the passive isolator is derived through solid approximations, and the fundamental frequency or performance limit is obtained using nonlinear analysis, which entirely explains the nonlinear behavior of the isolator. In addition, the approximate design equations of the isolator are derived to analyze its performance limit. Finally, an approximate expression of the lowest fundamental frequency of the isolator is derived using nonlinear analysis and design equations, which provide substantial design guidelines to improve isolator performance.

Keywords: Negative stiffness mechanism; Nonlinear vibration; Passive vibration isolator; Performance limit

1. Introduction

Vibration criteria for vibration-sensitive equipment have become stricter due to greater precision and a continuing need to minimize production defects in microelectronic, medical, and biopharmaceutical industries. In addition, these trends in vibration criteria will continue into the future, considering the rapid development of nanotechnology. Therefore, local vibration isolation systems are necessary for precision and vibration sensitive objects, although anti-vibration techniques are already widely applied for building structures.

Passive isolators prevent vibration transmission by reducing its stiffness, and pneumatic passive isolators are most widely used. Recently, several isolators based on a zero-compliance mechanism have been proposed and are replacing the pneumatic passive isolators [1-5]. In particular, a passive vibration isolator using a negative stiffness mechanism (NSM), as shown in Fig. 1, is being considered for small precision instruments.

Since the passive isolator using the NSM does not need any external power supply or pressurized air,

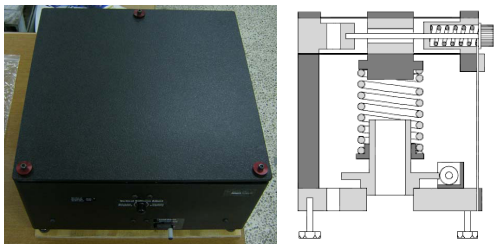

(a) Photo (b) Schematic

Fig. 1. The vertical isolator using NSM [3, 4].

† This paper was recommended for publication in revised form by Associate Editor Seong-Wook Hong

*Corresponding author. Tel.: +82 2 820 0654, Fax.: +82 2 820 0668
E-mail address: ahj123@ssu.ac.kr

maintenance efforts can be significantly reduced. Moreover, the isolation efficiency of the isolator is much better than that of an ordinary pneumatic isolator since the fundamental frequency of the isolator can be lowered to 0.5 Hz. However, the systematic design procedure of the NSM is not fully revealed even though the working principle of the NSM and its patents are well known [3-4]. In addition, the isolator shows a nonlinear behavior as the fundamental frequency is lowered. Nevertheless, the nonlinear behavior of the isolator cannot be explained with a linear model. Furthermore, there is no literature on the lowest fundamental frequency that determines the isolation performance.

In this paper, the performance limit or the lowest fundamental frequency of the passive vertical isolator using the NSM is discussed, and the design guidelines of the isolator are presented. First, the approximate governing equation of the passive isolator is shown to be the well-known Duffing equation, and the lowest fundamental frequency is obtained through the nonlinear analysis of the dynamic model. The derived nonlinear model can completely explain the nonlinear behavior and tells us how to determine the lowest fundamental frequency of the isolator. Approximate design equations for the isolator are derived to analyze the performance limit of the isolator. Finally, the performance limit or the lowest fundamental frequency of the isolator is derived using the results of the nonlinear analysis and the design equations.

2. Nonlinear model and analysis of the passive isolator using NSM

2.1 Nonlinear dynamic model

The vertical isolator of Fig. 1 can be simplified into mass, vertical spring, and NSM consisting of the notched flexures of length [L] and a compressive force [P]. The schematic of the vertical isolator is shown in Fig. 2.

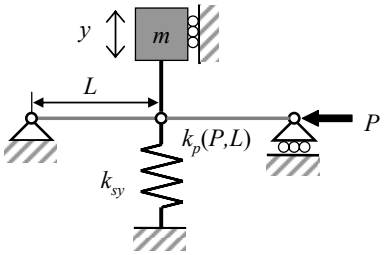

Fig. 2. Schematic of the vertical isolator.

The equation of motion of the isolator can be expressed as

$$m\ddot{y} + (k_{sy} + k_p)y = 0 \tag{1}$$

where k_{sy} is the stiffness of the vertical spring and $k_p(P, L)$ is the stiffness of the NSM.

The stiffness of the NSM [$k_p(P, L)$] can be approximated as the sum of the stiffness of the notched flexure under zero compressive force [k_{p0}] and the negative stiffness due to the compressive force [$-P/L$] as shown in Eq. (2). A small motion [Δy] of the mass produces additional moment load [$P\Delta y$] due to the compressive force, and the moment load makes the flexure deflect further, which means the negative stiffness. The exact stiffness of a beam under a compressive force has a complex form of trigonometric functions, and the equivalent length of the notched flexure depends on its deformation [6-7]. Since the exact stiffness of the notched flexure cannot give us any physical insight, the approximate expression is used to derive a nonlinear model. The compressive force is generated by initially deforming a horizontal spring of the stiffness [k_{sp}] up to some displacement [x_0] such as $P = k_{sp}(x_0 + x_p)$.

$$k_p(P,L) \approx k_{p0} - \frac{P}{L} \tag{2}$$

The parasitic X-directional motion [x_p] is generated by the Y-directional deformation of the notched flexure, and the parasitic motion is approximately expressed as Eq. (3).

$$x_p = -\frac{2y^2}{L + \sqrt{L^2 - y^2}} \approx -\frac{y^2}{L} \tag{3}$$

Considering both the compressive force generation of a horizontal spring and the parasitic motion, the modified schematic of the vertical isolator is shown in Fig. 3. The resulting dynamic model of the vertical isolator is shown in Eq. (4).

$$m\ddot{y} + (k_{sy} + k_{p0} - k_{sp}\frac{x_0}{L} + k_{sp}\frac{y^2}{L^2})y = 0 \tag{4}$$

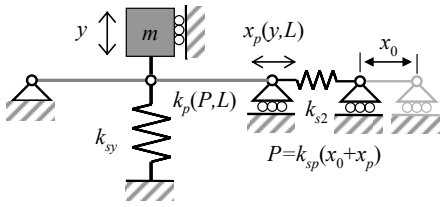

Fig. 3. Schematic of the vertical isolator considering the parasitic motion.

Simplifying Eq. (4) by introducing the equivalent stiffness [k_{eq} (= k_{sy} + k_{p0} - $k_{sp}x_0/L$)], the resulting equation of motion can be expressed by Eq. (5), which is the well-known Duffing equation with a nonlinear cubic stiffness.

$$m\ddot{y} + k_{eq}y + k_{sp}\frac{y^3}{L^2} = 0 \tag{5}$$

2.2 Nonlinear analysis

2.2.1 Equilibrium points

The equilibrium points of Eq. (5) can be obtained by making the differential term zero and solving the remaining algebraic equation. The resulting equilibrium points of the equation of motion depend on the value of the equivalent stiffness [k_{eq}] as shown in Eq. (6)

$$y_{eq} = \begin{cases} 0 & ,k_{eq} \geq 0 \\ 0, \pm L\sqrt{\dfrac{-k_{eq}}{k_{sy}}} & ,k_{eq} < 0 \end{cases} \tag{6}$$

The normalized equilibrium points [y_{eq}/L] according to the normalized equivalent stiffness [k_{eq}/k_{sy}] are shown in Fig. 4. If the equivalent stiffness is larger than zero, the governing equation has only one equilibrium point at $y = 0$. On the other hand, if the equivalent stiffness becomes negative, the governing equation has three equilibrium points.

Stabilities of the equilibrium points can be determined by inspecting the eigenvalues of the linearized system at the equilibrium points. If the real part of the eigenvalue is positive, the corresponding equilibrium point is unstable. The eigenvalues and the corresponding equilibrium points are shown in Eq. (7). If the equivalent stiffness is larger than zero [$k_{eq} \geq 0$], the linearized system has stable conjugate eigenvalues, and the equilibrium point at $y = 0$ is stable. Therefore, the system response will finally converge at the equilibrium point. On the other hand, the system has one unstable equilibrium point at $y = 0$ and two stable equilibrium points at $y = \pm L\sqrt{-k_{eq}/k_{sy}}$ as the equivalent stiffness becomes negative. That is, the equilibrium point at $y = 0$ becomes unstable, and two new stable equilibrium points appear as the equivalent stiffness becomes negative. Therefore, the system response will finally converge, not at the equilibrium point of $y = 0$, but at one of $y = \pm L\sqrt{-k_{eq}/k_{sy}}$.

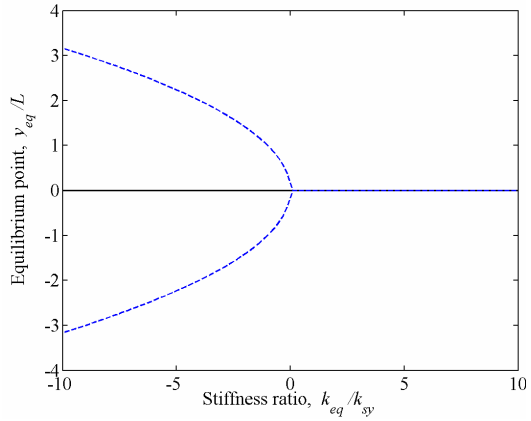

Fig. 4. Variations of the equilibrium points according to the equilibrium stiffness.

$$\lambda = \begin{cases} \pm j\sqrt{\dfrac{k_{eq}}{m}}\left(y_{eq}=0\right) & ,k_{eq} \geq 0 \\ \pm\sqrt{\dfrac{-k_{eq}}{m}}\left(y_{eq}=0\right), \pm j\sqrt{\dfrac{-2k_{eq}}{m}}\left(y_{eq}=\pm L\sqrt{\dfrac{-k_{eq}}{k_{sy}}}\right) & ,k_{eq} < 0 \end{cases} \tag{7}$$

Fig. 5 shows two vibration responses of a commercial minus-k vertical isolator [3-4]: positive equivalent stiffness [Fig. 5(a)] and negative equivalent stiffness [Fig. 5(b)]. The responses shown in Fig. 5 are different from those of an ordinary linear vibration in several points. First, the vibration period of Fig. 5(a) becomes longer as time elapses, and the response decreases. This can be explained by the cubic stiffness of Eq. (5). Second, the equilibrium point of Fig. 5(b) is far from $y = 0$, and the response is not symmetric to the equilibrium point, while the response of Fig. 5(a) converges to zero and is symmetric to the X-axis as described in Eq. (7). The nonlinear behaviors of the vertical isolator can be fully described by this newly-derived nonlinear model.

Since the equilibrium point should not be changed, the best isolation performance or the lowest fundamental frequency of the isolator can be achieved at the transition point where the sign of the equivalent stiffness changes from positive to negative. In the next section, the fundamental frequency of the nonlinear model will be determined though nonlinear vibration analysis.

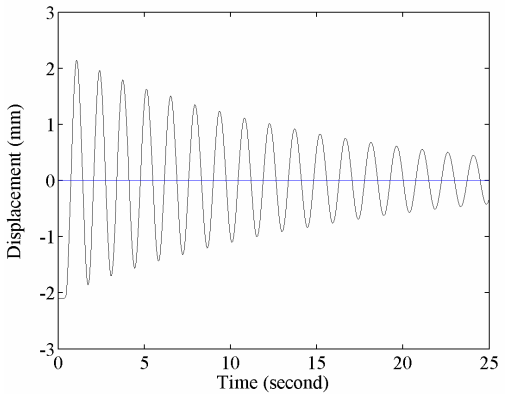

(a) Positive equivalent stiffness

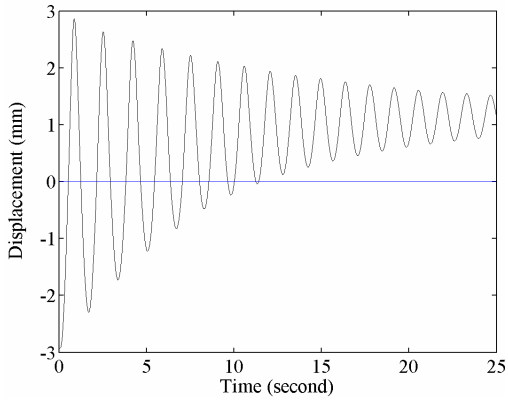

(b) Negative equivalent stiffness

Fig. 5. Vibration responses according to the equilibrium point change.

2.2.2 Lowest fundamental frequency

The free vibration response and fundamental frequency of the nonlinear equation of motion are derived using a perturbation method. For convenience, some variables of Eq. (4) are replaced with new variables, and the resulting equation is shown in Eq. (8).

$$\ddot{y} + \omega_0^2 y + \varepsilon\omega_0^2 y^3 = 0 \tag{8}$$

where $k_{eq}/m = \omega_0^2$, $k_{sp}/m = \omega_{sp}^2$ and $\varepsilon\omega_0^2 = \omega_{sp}^2/L^2$, and ε is the small perturbation.

The vibration response and the fundamental frequency of Eq. (8) can be expressed by the power series of the small perturbation [ε] as shown in Eq. (9).

$$\begin{aligned} \omega &= \omega_0 + \varepsilon\omega_1 + \varepsilon^2\omega_2 + \cdots \\ y &= y_0 + \varepsilon y_1 + \varepsilon^2 y_2 + \cdots \end{aligned} \tag{9}$$

Lindstedt's method is then employed to suppress the secure terms for every order. The fundamental frequency for the second order approximation can be derived as Eq. (10) [8].

$$\omega = \omega_{eq}\left(1 + \varepsilon\frac{3}{8}A^2 - \varepsilon^2\frac{21}{256}A^4\right) \tag{10}$$

where A [$= y(0)$] is the initial displacement at $t = 0$.

After squaring both sides of Eq. (10) and substituting the original parameters for the small perturbation [ε], the lowest fundamental frequency can be approximated as Eq. (11) in that the initial deformation [A] is far less than the notched flexure length [L]. The lowest fundamental frequency is related to the stiffness of the horizontal spring for the compressive force [k_{sp}], initial deformation [A], and length [L] of the notched flexure.

$$\omega^2 \approx \frac{3}{4}\frac{\omega_{sp}^2}{L^2}A^2 \tag{11}$$

Notice that the lowest fundamental frequency of the isolator is governed not by the vertical coil spring [k_{sy}] but by the horizontal spring for a compressive force [k_{sp}]. That is, since the stiffness of the vertical coil spring is balanced by the negative stiffness of the flexure, the nonlinear cubic stiffness term of Eq. (5) determines the lowest fundamental frequency. The lowest fundamental frequency of the isolator indicates the isolation performance: lower fundamental frequency gives better isolation efficiency. At first glance, the fundamental frequency can be lowered by reducing the horizontal spring stiffness and initial deformation, and increasing the notched flexure length. However, there must be a relationship between the initial deformation [A] and the notched flexure length [L] if the initial deformation is assumed to be a function of the maximum deformation. Therefore, the fundamental frequency should be determined by considering the relationship between the maximum deformation and the notched flexure length.

3. Approximate design equations for a passive isolator using the NSM

3.1 Design considerations

3.1.1 Maximum deformation

The total load of the notched flexure by both the deformation and the compressive force should be within the fatigue failure strength. The symmetric vertical force [F] is introduced for only the translation motion of the notched flexure as shown in Fig. 6. Since the

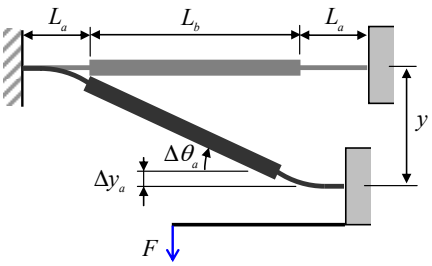

Fig. 6. The notched flexure.

deformation of the thick part *b* is far less than that of the notched part *a*, the total vertical deformation can be expressed by

$$y = 2\Delta y_a + \Delta\theta_a L_b \tag{12}$$

The stiffness of the notched flexure (Fig. 6) [k_{p0}] without any compressive force can be expressed by Eq. (13) considering a simple beam theory under moment and force loads.

$$k_{p0} = \frac{F}{y} = \frac{EI}{\left(\frac{2}{3}L_a^3 + L_a^2 L_b + \frac{1}{2}L_a L_b^2\right)} \tag{13}$$

The maximum force due to the maximum deformation of the notched flexure is determined by the product of the stiffness [k_{p0}] and the maximum deformation [y_{max}]. The location of the maximum moment is the end of the notched flexure, and the value can be approximately expressed by Eq. (14). The exact expression of the moment of the notched flexure under a compressive force is a very complex form of trigonometric functions, and the exact value can be obtained only by numerical calculation [6, 7]. Moreover, the location and the value of the maximum moment depend on the compressive force and deformation of the flexure.

$$M_{\max} = k_{p0} y_{max}(L_a + \frac{L_b}{2}) \tag{14}$$

Since a large compressive force is required to balance the equivalent stiffness, the compressive force as well as the moment of Eq. (14) should be considered in the stress analysis. The total stress fluctuates according to the isolator oscillation due to the moment and compressive force. The stress due to the compressive force is the static component, while the stress due to the moment is the alternating component [9]. If the height and width of the notched part of the flexure are *h* and *w*, respectively, the fatigue diagram of the Soderberg line can be expressed by Eq. (15).

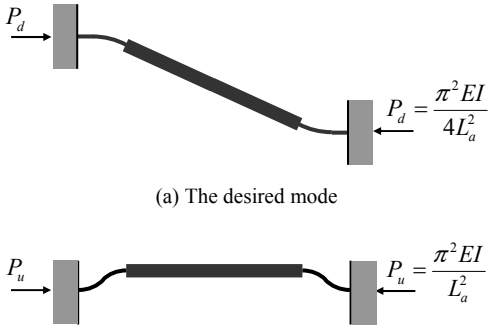

(a) The desired mode

(b) The undesired mode

Fig. 7. The buckling modes.

$$\frac{S_\sigma}{\sigma_e}\frac{Ey_{max}(L_a + \frac{L_b}{2})}{\left(\frac{2}{3}L_a^3 + L_a^2 L_b + \frac{1}{2}L_a L_b^2\right)}\frac{h}{2} + \frac{S_\sigma}{\sigma_y}\frac{P}{wh} \le 1 \tag{15}$$

where σ_e and σ_y are the endurance limit and the yield stress of the flexure material, respectively, and S_σ is the safety factor considering stress concentration.

3.1.2 Buckling due to compressive force

The buckling mode of the notched flexure in Fig. 7(a) is desirable and the compressive force accelerates this buckling mode to produce the negative stiffness. Since part *b* is thick enough to be regarded as rigid, only the buckling condition of the notched part is considered. In case of Fig. 7(a), the boundary condition of the notched part is one end free and the other end fixed [Eq. (16a)]. On the other hand, the undesired buckling mode in Fig. 7(b) has a boundary condition of both ends fixed [Eq. (16b)]. Therefore, the compressive force satisfies both inequalities of Eq. (16c), considering both the buckling modes and safety factor [S_b] in Fig. 7 [9].

$$\frac{\pi^2 EI}{4L_a^2} \le P \tag{16a}$$

$$P \le \frac{\pi^2 EI}{L_a^2} \tag{16b}$$

$$\frac{\pi^2 EI}{4L_a^2} \le P \le \frac{\pi^2 EI}{S_b L_a^2} \tag{16c}$$

3.1.3 Required compressive force

As mentioned in section 2.2.1, the lowest fundamental frequency can be achieved by an appropriate compressive force, which is large enough to compensate for the stiffness of both the vertical coil spring and flexure stiffness. The total stiffness of Eq. (1) can be expressed by (k_{sy}+ n k_p) if the number of flexure is n. Since the flexure stiffness [k_{p0}] without any compressive force in Eq. (2) is much smaller than the vertical coil spring stiffness [k_{sy}], the flexure stiffness [k_{p0}] without any compressive force is neglected for simplicity. Then, the compressive force should be large enough to make the total stiffness less than zero as Eq. (17) to lower the fundamental frequency.

$$k_{total} = k_{sy} + n \cdot k_p(P,L) \approx k_{sy} - \frac{nP}{2L_a + L_b} \le 0 \quad (17)$$

3.2 Derivation of the design equations

If part b of the notched flexure is t times longer than part a of the notched flexure [$L_b = tL_a$], design equations are derived for the design parameters to satisfy the three inequalities in section 3.1. First, Eq. (16b) can be expressed by Eq. (18a) considering the area moment of inertia [I] is $wh^3/12$, and Eq. (17) can be rewritten as Eq. (18b) considering $L_b = tL_a$.

$$P \le \frac{\pi^2 EI}{S_b L_a^2} = \frac{\pi^2 E}{12 S_b} \frac{wh^3}{L_a^2} \quad (18a)$$

$$P \ge k_{sy} \frac{L_b + L_a}{n} = k_{sy} \frac{(t+2)L_a}{n} \quad (18b)$$

The two inequalities related to the compressive force [P], Eqs. (18a) and (18b), are combined as Eq. (19).

$$k_{sy} \frac{(t+2)L_a}{n} \le P \le \frac{\pi^2 E}{12 S_b} \frac{wh^3}{L_a^2} \quad (19)$$

Since the upper bound of the compressive force should be bigger than the lower bound, an inequality related to the length of the notched part [L_a] can be derived, and the inequality finally results in the upper bound of the length of the notched part [L_a] as shown in Eq. (20).

$$k_{sy} \frac{(t+2)L_a}{n} \le \frac{\pi^2 E}{12 S_b} \frac{wh^3}{L_a^2} \rightarrow L_a^3 \le \frac{\pi^2 E}{12 S_b k_{sy}} \frac{nwh^3}{(t+2)} \quad (20)$$

For simplicity, the yield strength is assumed to be twice the endurance limit [$\sigma_y = 2\sigma_e$] and the thick part b much longer than the notched part a [$L_b >> L_a$]. The first term of Eq. (15) can then be rewritten as (21a), neglecting the cubic terms of L_a in the denominator. In addition, the second term of Eq. (15) can be rewritten as Eq. (21b) by substituting the maximum compression force of Eq. (19).

$$\frac{S_\sigma}{\sigma_e} \frac{Ey_{max}(L_a + \frac{L_b}{2})}{\left(\frac{2}{3}L_a^3 + L_a^2 L_b + \frac{1}{2}L_a L_b^2\right)} \frac{h}{2} \approx \frac{2S_\sigma}{\sigma_y} \frac{Ey_{max}(L_a + \frac{L_b}{2})}{\left(L_a^2 L_b + \frac{1}{2}L_a L_b^2\right)} \frac{h}{2} = S_\sigma h \frac{E}{\sigma_y} \frac{y_{max}}{tL_a^2} \quad (21a)$$

$$\frac{S_\sigma}{\sigma_y} \frac{P}{wh} = \frac{S_\sigma}{\sigma_y} \frac{1}{wh} \frac{\pi^2 E}{12 S_b} \frac{wh^3}{L_a^2} = S_\sigma h \frac{E}{\sigma_y} \frac{\pi^2 h}{12 S_b L_a^2} \quad (21b)$$

Therefore, the lower limit of the notched part length [L_a] can be obtained as Eq. (22) since the sum of Eq. (21a) and (21b) should be less than one considering the fatigue condition of Eq. (15).

$$S_\sigma h \frac{E}{\sigma_y} \left(\frac{y_{max}}{t} + \frac{\pi^2 h}{12 S_b} \right) \le L_a^2 \quad (22)$$

By combining the two inequalities related to the notched part length [L_a], Eqs. (20) and (22), a complete inequality related to the notched part length can be derived as Eq. (23).

$$\sqrt{S_\sigma h \frac{E}{\sigma_y} \left(\frac{y_{max}}{t} + \frac{\pi^2 h}{S_b 12} \right)} \le L_a \le h \sqrt[3]{\frac{\pi^2 E}{12 S_b k_{sy}} \frac{nw}{(t+2)}} \quad (23)$$

Since the lower bound of Eq. (23) should be less than its upper bound for there to be a proper value of the notched part length, the minimum thickness [h] of the notched part a can be derived using Eq. (23) as well. Assuming that maximum deformation [y_{max}] is much larger than the thickness [h] for a small isolator, we can further simplify the minimum thickness of the notched part as Eq. (24).

Therefore, if the vertical spring stiffness, safety factors, and the number and width of the notched flexure are given, the shape of the notched flexure can be de-

$$\sqrt{S_\sigma h \frac{E}{\sigma_y} \left(\frac{y_{max}}{t} + \frac{\pi^2 h}{S_b 12} \right)} \le h \sqrt[3]{\frac{\pi^2 E}{12 S_b k_{sy}} \frac{nw}{(t+2)}} \rightarrow \frac{S_\sigma y_{max}}{\sigma_y} \sqrt[3]{\frac{144 S_b^2 E k_{sy}^2}{\pi^4} \frac{(t+2)^2}{t^3 n^2 w^2}} \le h \quad (24)$$

Table 1. Design equations of the vertical isolator.

Values	Design equation
h	$\frac{S_\sigma y_{max}}{\sigma_y}\sqrt[3]{\frac{144S_b{}^2Ek_{sy}{}^2}{\pi^4}\frac{(t+2)^2}{t^3n^2w^2}}$
L_a	$\frac{S_\sigma y_{max}}{\sigma_y}\sqrt[3]{\frac{12S_bk_{sy}}{\pi^2}\frac{(t+2)}{t^3nw}}$
P	$\frac{S_\sigma y_{max}}{\sigma_y}\sqrt[3]{\frac{12S_bk_{sy}{}^4}{\pi^4}\frac{(t+2)}{n^4w}}$

termined from the design equations, which are summarized in Table 1.

4. Lowest fundamental frequency of the vertical isolator

Assuming that the initial deformation [A] is equal to the maximum deflection [y_{max}] and substituting the design equation related to the notched flexure length in Table 1 for Eq. (11), the lowest fundamental frequency can be rewritten as

$$\omega^2 \approx \frac{3}{4}\frac{\omega_{sp}{}^2}{L^2}A^2 = \frac{3}{4}\omega_{sp}{}^2\frac{\sigma_y{}^2}{S_\sigma{}^2}\sqrt[3]{\frac{\pi^4n^2w^2}{144S_b{}^2k_{sy}{}^2}\frac{t^6}{(t+2)^8}} \quad (25)$$

The approximate expression of the lowest fundamental frequency or Eq. (25) reveals meaningful design guidelines to improve the isolator performance. The most important parameter is the horizontal spring, the stiffness of which should be kept as small as possible, while it is better for the vertical spring to be very stiff. The number and width of the notched flexure should be minimized to enlarge the length of the notched flexure, which can lower the fundamental frequency of the isolator.

5. Conclusion

This paper discussed the performance limit of the passive vertical isolator using the NSM and presents the design guidelines of the isolator based on the performance limit. First, the approximate dynamic model of the passive isolator was shown to be the well known Duffing equation, and the nonlinear analysis of the dynamic model resulted in a performance limit or the lowest fundamental frequency of the isolator. The nonlinear behavior of the isolator and the performance limitation were fully explained by the derived nonlinear model. An approximate expression of the performance limit or the lowest fundamental frequency of the isolator was derived using the results of the nonlinear analysis and the design equations. The result showed meaningful design guidelines to improve the isolator performance.

Acknowledgement

This work was supported by the Soongsil University Research Fund.

References

[1] A. Carrella, M. J. Brennan and T. P. Waters, Optimization of a Quasi-Zero-Stiffness Isolator, *Journal of Mechanical Science and Technology* 21 (6) (2007) 946-949.

[2] T. Mizuno, T. Toumiya and M. Takasaki, Vibration isolation system using negative stiffness *JSME international Journal C*, 46 (3) (2003) 807-812.

[3] D. L. Platus, Smoothing out bad vibes, *Machine design*, (1993) Feb. 123-130.

[4] D. L. Platus, Negative-stiffness-mechanism vibration isolation systems *SPIE conference on Current Developments for Optomechanical systems*, Denver, Colorado, USA, 3786 (1999).

[5] J. Zhang, D. Li and S. Dong, An ultra-low frequency parallel connection nonlinear isolator for precision instruments, *Key Engineering Materials* 257-258 (2004) 231-236.

[6] S. T. Smith, *Flexures*, Gordon and Breach, London and New York (2000).

[7] J. U. Chang, *A Study on an active sub-hertz vibration isolator design and control*, Ph.D thesis, Seoul National University (2007).

[8] L. Meirovitch, *Fundamentals of vibrations*, McGraw-Hill, New York, USA, (2001).

[9] J. E. Shigley and C. R. Mischke, *Mechanical Engineering Design* 6ed, McGraw-Hill, New York, USA, (2001).

Dr. Ahn received B. S., M. S. and Ph. D. degrees from Seoul national university in 1995, 1997 and 2001, respectively. Dr. Ahn was a research associate of University of Virginia, USA and worked as a BK21 assistant professor at Seoul national university. Dr. Ahn is currently an assistant professor at department of mechanical engineering at Soongsil University. He is currently serving as an editor of the International Journal of Rotating Machinery. Dr. Ahn's research interests are in the area of rotordynamics, control and mechatronics.